High Order Workshop Results for Case 3.2 Turbulent Flow over DPW3 Wing

Michael J. Brazell * and Dimitri J. Mavriplis †

Department of Mechanical Engineering, University of Wyoming, Laramie WY 82071, USA

I. Code Description

A 3D Discontinuous Galerkin (DG) finite element method[1] is used to discretize the compressible Navier-Stokes (CNS) equations. The solver can handle hybrid mixed element meshes (tetrahedra,pyramids,prisms, and hexahedra), curved elements, and incorporates both p-enrichment and h-refinement capabilities using non-conforming elements (hanging nodes). Additional equations that can be solved include a PDE-based artificial viscosity equation[2–4] and the Spalart-Allmaras turbulence model (negative-SA variant).[5] The implicit solver uses a Newton-Raphson method to solve the non-linear set of equations. These equations are linearized to obtain the full Jacobian. The linear system is solved using a flexible-GMRES[6] (fGMRES) method. To further improve convergence of fGMRES a preconditioner can be applied to the system of equations. Preconditioners that have been implemented include Jacobi relaxation, Gauss-Seidel relaxation, line implicit Jacobi, and ILU(0). The solver is parallelized using MPI.

II. Case Summary

Steady state solutions of turbulent flow. In these cases the negative-Spalart-Allmaras[5] turbulence model is used. The non-linear residual is driven down 8 orders of magnitude using the implicit Newton-Rhapson solver.

A. Hardware

Simulations were performed on the NCAR-Wyoming supercomputer (NWSC) Yellowstone which is a 1.5 Petaflops high performance IBM iDataPlex architecture featuring 72,576 Intel Sandybridge cores (2.6 GHz Intel E5-2670 processors configured in dual socket nodes) and 144.6 TB of memory. The Taubench for this machine is 8.4 seconds.

III. Meshes

The provided curved hexahedral grids will be used. Although this grid is built using a surface defined with b-splines it is easy to show that the cubic elements to not preserve curvature, which can lead to jumps in pressure. This is most likely due to the grid points not aligning with the control points in the splines.

IV. Results

Solutions to flow over the DPW3 wing are discussed in this section. Due to the issues with the curvature of the grid no attempt was made to refine or adapt the grid. Simulations were carried out varying the polynomial degree and the artificial viscosity parameter κ, where larger κ causes larger artificial viscosity. The results for drag and lift coefficient are shown in Table 2. Based on the third drag prediction workshop:

*Post Doctoral Research Associate, AIAA Member

†Professor, AIAA Associate Fellow

the range of acceptable drag coefficient is $0.0185 \leq C_D \leq 0.0206$ and lift coefficient is $0.44 \leq C_L \leq 0.48$. Cases 1 and 2 ($p = 1, \kappa = 2, 1.75$) have too much viscosity and give poor predictions for lift and drag. Case 3 ($p = 1, \kappa = 1.5$) has just enough viscosity for stabilization and gives reasonable predictions for lift and improved drag. Case 4 ($p = 2, \kappa = 2$) again has too much viscosity and gives poor results but are better than Case 1 due to the increase in polynomial degree. Cases 5-7 all give lift and drag within acceptable ranges.

Figure 1 shows surface contours of pressure for Cases 2, 3, 5, and 7. The only solutions to have smooth contours of pressure are Case 1 (not shown in figure) and Case 2. These also give the worst predictions for lift and drag. The higher resolution and smaller values of artificial viscosity lead to non-smooth pressure contours but give better lift and drag predictions. The jumps in pressure are believed to be caused from the jumps in curvature between elements. The element mapping is a cubic $p = 3$ polynomial representation of a surface made of cubic B-splines. However, the elements do not align with the control points for the splines. Therefore this mesh is only piecewise continuous and both the slopes and curvature are discontinuous between elements. Figure 2 shows surface contours of artificial viscosity for Cases 2, 3, 5, and 7. Cases 2 and 3 have a lot of artificial viscosity within the domain due to under resolution of the solution causing large jumps in pressure. Cases 5 and 7 however show artificial viscosity primarily on the wing surface, most likely due to the grid. Figure 3 shows surface contours of eddy viscosity for Cases 2, 3, 5, and 7. Case 2 is over predicting eddy viscosity and has jumps within the wake. Case 3 has a more accurate eddy viscosity with smaller jumps. Cases 5 and 7 show accurate eddy viscosity and smoother solutions.

It is shown in these results that too much artificial viscosity may give smooth solutions but can lead to poor predictions for lift and drag. Also, discontinuities of curvature on the wing surface can lead to large pressure fluctuations. In order to get accurate solutions for the DPW3 wing a new high order grid is needed and with enough resolution solutions without artificial viscosity may be obtained.

Table 1. Drag and lift coefficients for varying polynomial degree p and artificial viscosity parameter κ

case	p	κ	C_D	C_L
1	1	2	0.05271	0.1056
2	1	1.75	0.03747	0.0974
3	1	1.5	0.02332	0.4604
4	2	2	0.02247	0.3392
5	2	1.75	0.01961	0.4509
6	2	1.5	0.01955	0.4780
7	3	1.75	0.01932	0.4507

References

[1]Brazell, M. J. and Mavriplis, D. J., "3D mixed element discontinuous Galerkin with shock capturing," San Diego, CA, United states, 2013, pp. American Institute of Aeronautics and Astronautics (AIAA) –.

[2]Persson, P.-O. and Peraire, J., "Sub-cell shock capturing for discontinuous Galerkin methods," *Collection of Technical Papers - 44th AIAA Aerospace Sciences Meeting*, Vol. 2, 2006, pp. 1408 – 1420.

[3]Burgess, N., *An Adaptive Discontinuous Galerkin Solver for Aerodynamic Flows*, Ph.D. thesis, University of Wyoming, 2011.

[4]Barter, G. and Darmofal, D., "Shock capturing with PDE-based artificial viscosity for DGFEM: Part I. Formulation," *J. Comput. Phys. (USA)*, Vol. 229, No. 5, 2010/03/01, pp. 1810 – 27.

[5]Allmaras, S., Johnson, F., and Spalart, P., "Modifications and Clarifications for the Implementation of the Spalart-Allmaras Turbulence Model," *7th International Conference on Computational Fluid Dynamics*, 2012.

[6]Saad, Y., "A flexible inner-outer preconditioned GMRES algorithm," *SIAM J. Sci. Comput.*, Vol. 14, No. 2, March 1993, pp. 461–469.

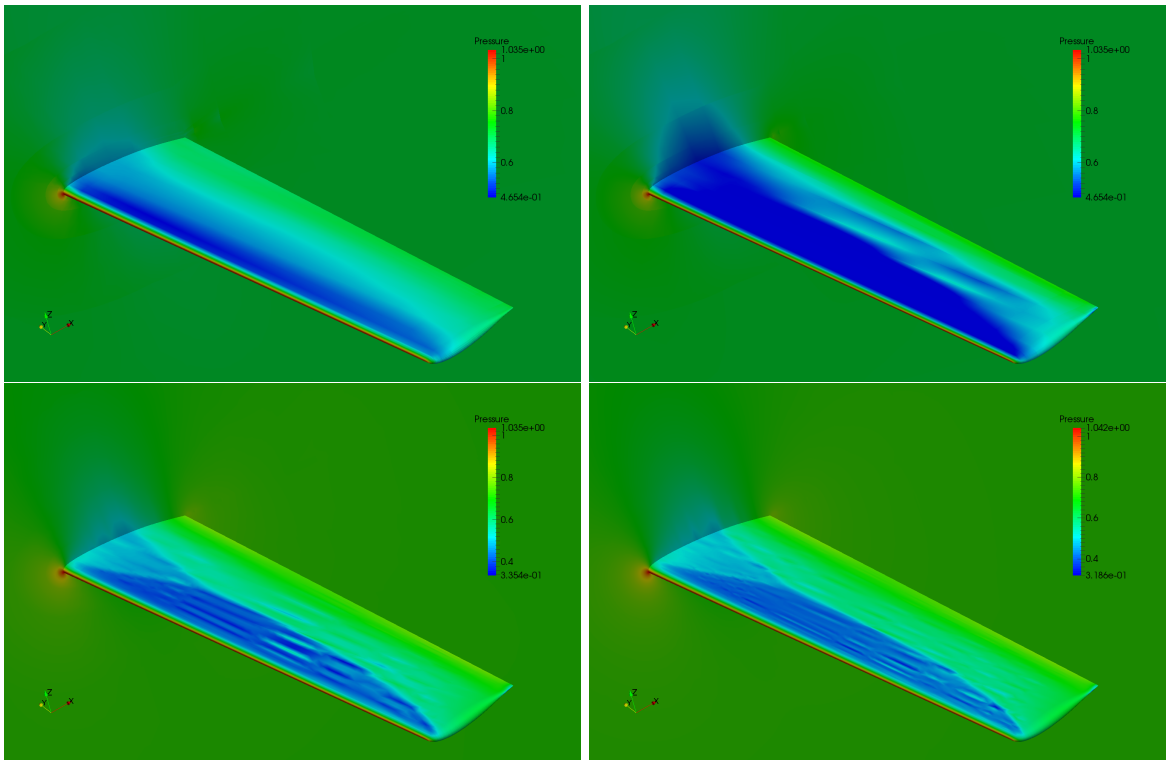

Figure 1. Contours of pressure for Case 2: $p = 1$, $\kappa = 1.75$ **(top left), Case 3:** $p = 1$, $\kappa = 1.5$ **(top right), Case 5:** $p = 2$, $\kappa = 1.75$ **(bottom left), Case 7:** $p = 3$, $\kappa = 1.75$ **(bottom right)**

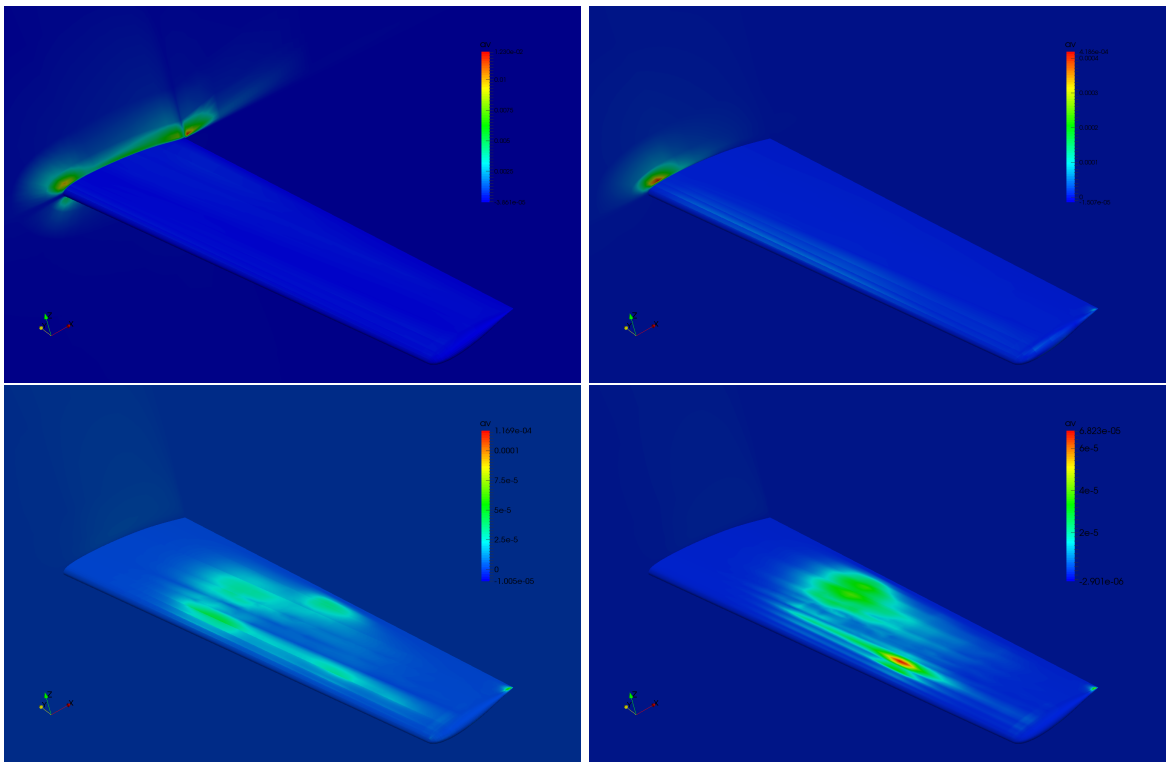

Figure 2. Contours of artificial viscosity for Case 2: $p = 1$, $\kappa = 1.75$ **(top left), Case 3:** $p = 1$, $\kappa = 1.5$ **(top right), Case 5:** $p = 2$, $\kappa = 1.75$ **(bottom left), Case 7:** $p = 3$, $\kappa = 1.75$ **(bottom right)**

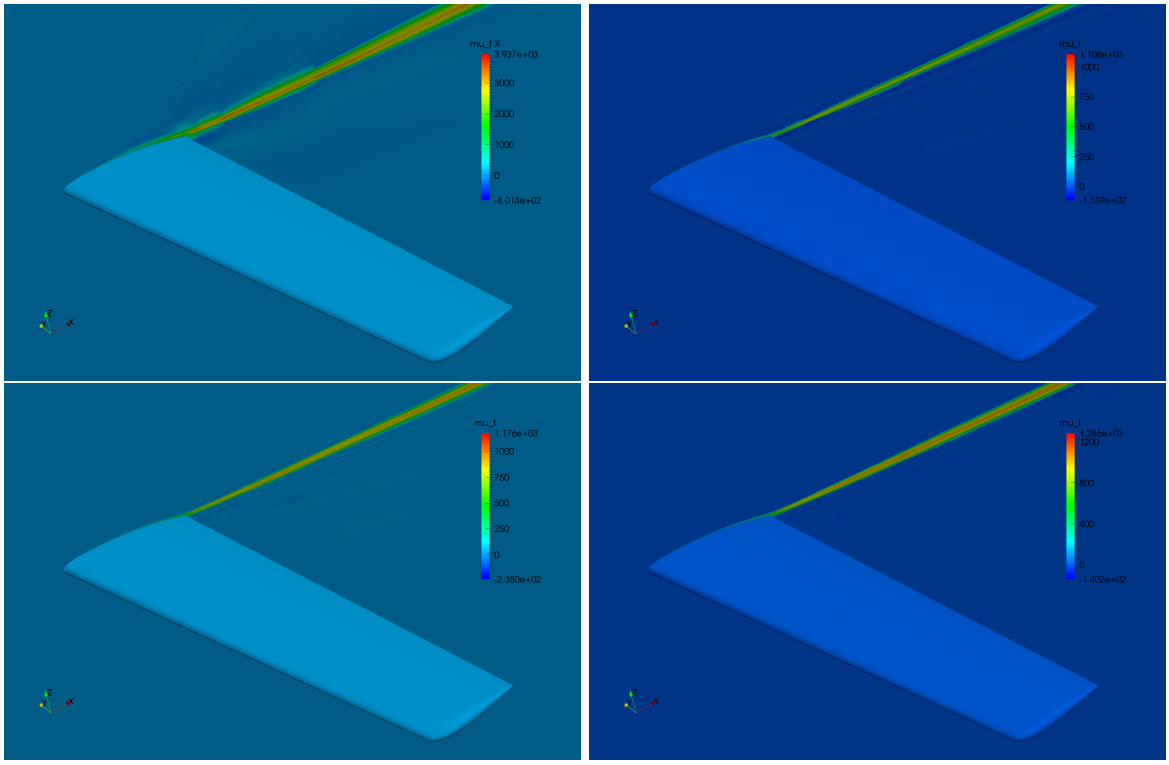

Figure 3. Contours of eddy viscosity for Case 2: $p = 1$, $\kappa = 1.75$ **(top left), Case 3:** $p = 1$, $\kappa = 1.5$ **(top right), Case 5:** $p = 2$, $\kappa = 1.75$ **(bottom left), Case 7:** $p = 3$, $\kappa = 1.75$ **(bottom right)**